ACS APPLIED MATERIALS & INTERFACES

Research Article

www.acsami.org

Femtosecond Nanostructuring of Glass with Optically Trapped Microspheres and Chemical Etching

A. Shakhov,[*,†,‡] A. Astafiev,[‡] A. Gulin,[‡,§] and V. Nadtochenko[‡,§,⊥]

[†]Moscow Institute of Physics and Technology, Institutskiy lane 9, Dolgoprudny, Moscow Region 141700, Russian Federation

[‡]Semenov Institute of Chemical Physics RAS, Kosygina st. 4, Moscow 119991, Russian Federation

[§]Department of Chemistry, Moscow State University, GSP-1, Leninskiye Gory 1-3, Moscow 119991, Russian Federation

[⊥]Institute of Problems of Chemical Physics RAS, Academician Semenov avenue 1, Chernogolovka, Moscow Region 142432, Russian Federation

Supporting Information

ABSTRACT: Laser processing with optically trapped microspheres is a promising tool for nanopatterning at subdiffraction-limited resolution in a wide range of technological and biomedical applications. In this paper, we investigate subdiffraction-limited structuring of borosilicate glass with femtosecond pulses in the near-field of optically trapped microspheres combined with chemical postprocessing. The glass surface was processed by single laser pulses at 780 nm focused by silica microspheres and then subjected to selective etching in KOH, which produced pits in the laser-affected zones (LAZs). Chemical postprocessing allowed obtaining structures with better resolution and reproducibility. We demonstrate production of reproducible pits with diameters as small as 70 nm ($\lambda/11$). Complex two-dimensional structures with 100 nm ($\lambda/8$) resolution were written on the glass surface point by point with microspheres manipulated by optical tweezers. Furthermore, the mechanism of laser modification underlying selective etching was investigated with mass spectrum analysis. We propose that the increased etching rate of laser-treated glass results from changes in its chemical composition and oxygen deficiency.

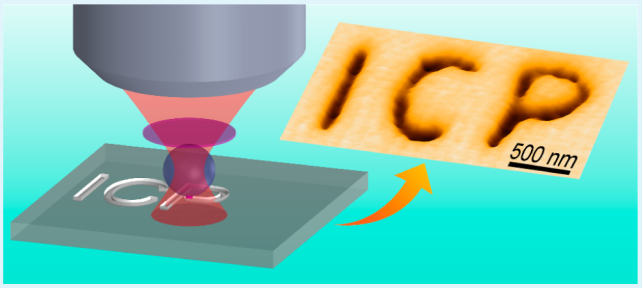

KEYWORDS: *nanostructuring, near-field, dielectric microspheres, optical trap, femtosecond lasers, laser-assisted chemical etching, TOF-SIMS, AFM*

INTRODUCTION

Ultrafast lasers are an excellent tool for structuring bulk transparent materials in a wide scope of applications. Large 2D and 3D structures can be easily produced by femtosecond pulses with resolution down to hundreds of nanometers. Spatial resolution is always a concern in laser structuring and is restricted by the diffraction limit. Resolution can be improved using multiphoton absorption of femtosecond pulses,[1,2] near-field effects,[3−10] and etching agents.[11]

Near-field effects can be provided by use of sharp AFM metal tips[5,12] or metal nanoparticles[13,14] illuminated by laser radiation. Another approach to near-field structuring involves dielectric microspheres with diameter on the order of 1 μm acting as small lenses. In some papers a monolayer of dielectric microspheres laid on the sample surface was exposed to femtosecond laser radiation, producing a hexagonal array of holes or bumps.[15] Other studies[16,17] show optical trapping of microspheres in liquid media and direct writing of subdiffraction-limited patterns on the surface. This method is more flexible compared with the use of a static monolayer because optical manipulation of trapped microspheres allows writing arbitrary patterns on the surface.

Whereas laser processing is mostly performed as a one-step direct-write procedure, it also can be realized with femtosecond laser irradiation and chemical etching (FLICE);[18,19] this technique is widely used in microfluidic applications.[20,21] Typical etching agents for treatment of various types of glasses are HF or KOH solutions. It has been demonstrated that KOH solution has lower etching speed but higher selectivity in comparison to HF in the formation of microchannels in fused silica.[21−23]

In this study we use amplified femtosecond laser pulses focused by silica microspheres on the borosilicate glass surface and carry out alkali postprocessing, which yields distinct craters in the laser-affected zones (LAZs). To enable writing of arbitrary surface patterns, microspheres were trapped and manipulated in aqueous media by optical tweezers. Moreover, to investigate the mechanism of laser modification we carry out mass spectroscopy analysis of LAZs in fused silica glass, which behaves in a similar way to borosilicate glass under laser

Received: October 6, 2015
Accepted: November 24, 2015
Published: November 24, 2015

DOI: 10.1021/acsami.5b09454
ACS Appl. Mater. Interfaces 2015, 7, 27467−27472

exposure but has a simpler chemical composition. Glass was chosen as a target material because well-known properties, transparency over a wide spectral range and thermal and electrical stabilities, make it an advantageous material for many practical applications.

EXPERIMENTAL SECTION

Femtosecond pulses at 80 MHz repetition rate from a Ti:sapphire oscillator (Spectra-Physics Tsunami) passed through a Pockels cell, switched by a TTL signal, and then passed through a custom-made four-pass amplifier. Output pulses had energy up to 4 μJ and spectral full width at half maximum (FWHM) of 32 nm at 780 nm central wavelength. Laser diode radiation (827 nm CW, Mitsubishi ML60171C) and femtosecond pulses were coupled to the Olympus IX71 research microscope and focused by objective lens (40× 0.75 N.A.) in a water solution containing 1.15 or 2.25 μm silica microspheres. Water as medium with high band gap, low viscosity, and high heat capacity provided effective optical trapping of microspheres. Both Brunauer–Emmett–Teller (BET) and measurements of microsphere sink speed in water indicated that they are nearly solid with negligible porosity. A single microsphere was drawn into the center of the laser diode beam and became optically trapped and was placed in contact with the sample surface. A programmable 3-D piezo stage was used for positioning of the microsphere into an appropriate point near the sample surface. Single amplified femtosecond pulses (780 nm, 30 fs) were demagnified with a system of lenses and coupled to the objective lens so that only a part of the objective entrance pupil was filled, which resulted in large waist radius (about 3.5 μm) and nearly a uniform field over the microsphere. Such an arrangement allowed us to avoid the need for accurate matching of two beams at a focal point. The femtosecond pulse was additionally focused by the trapped microsphere in its near-field zone, and the glass surface was processed in the point of contact (Figure 1). Movements of the microsphere relative to the sample surface were controlled by software, which also triggered laser pulses so that the laser processing procedure repeated point by point yielded complex geometry surface patterns. Microsphere movement and sample processing were monitored in real time using a CCD camera (Sony ExWave) attached to the microscope. After laser processing, the sample was treated in 10 M KOH solution for 20 min at 90 °C, washed with isopropanol in an ultrasonic bath, and scanned with the AFM head.

A time-of-flight secondary ion mass spectrometer TOF-SIMS 5 (ION-TOF, Germany) was utilized to analyze samples. A pulsed focused beam of 30 keV Bi_3^+ cluster ions was focused at the 800 nm spot on the sample surface. Ion pulse duration was 35 ns. An area of 400 × 400 μm was scanned with a resolution of 512 × 512 pixels.

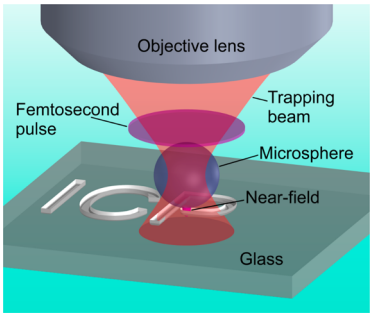

Figure 1. Scheme of optical trap assisted nanostructuring. Amplified femtosecond pulses were coupled to the objective lens, then they illuminated a silica microsphere and were focused in its near-field zone on the sample surface for laser nanoprocessing. The microsphere was trapped in water by a tightly focused CW laser beam.

RESULTS AND DISCUSSION

AFM imaging revealed the formation of sub-micrometer convex bumps on the glass surface in LAZs. We observed the following results of KOH treatment: (1) Bumps were completely etched, and craters were produced in their place (Figure 2a,b). (2) Whereas bumps were asymmetrical with much variation in shape from one bump to another, all craters produced by etching had highly regular circular shapes. (3) The FWHM of craters was invariably smaller than the same bumps' FWHM before etching (Figure 2c). Typically, bumps were about twice as wide as corresponding craters; only at minimal fluence was the difference smaller. Moreover, whereas the bumps shown in Figure 2c have an average width deviation equal to about 70 nm, the same deviation for craters produced after etching was 30 nm. Thus, chemical treatment resulted in more reproducible surface structures with more uniform lateral dimensions.

Therefore, the advantage of KOH treatment is in the formation of more uniform and regular structures with better spatial resolution and smoother surfaces compared with etching-free laser processing.

Glass structuring was strongly influenced by laser fluence in the focal spot. In previous works[20,24] three types of laser modification were observed in a glass: (a) refractive index alteration in the LAZ, (b) visible morphology alteration, and (c) disruptive modification with pronounced voids, cracks, etc.[20,25] In our experiments we mainly observed such modifications as bumps in LAZs and pits after KOH treatment. Laser-assisted etching produced surface structures discernible on the AFM image at fluence higher than a certain threshold value. The threshold was different for 1.15 and 2.25 μm spheres and equal to approximately 0.92 and 0.66 J/cm^2, respectively. For comparison, the same threshold determined from experiments where no microspheres were used and femtosecond pulses were tightly focused by the objective lens was several times larger (2.58 J/cm^2). We can understand this result as a

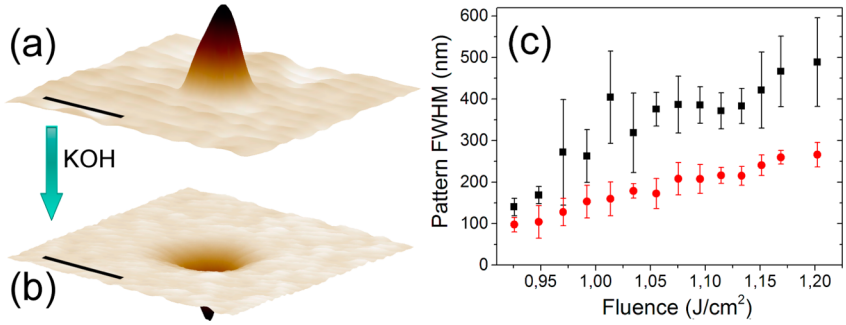

Figure 2. 3D view (a, b) and FWHM (c) of patterns formed in the LAZs with 1.15 μm SiO_2 microspheres on a glass surface before (a and c, black squares) and after (b and c, red circles) KOH treatment measured by AFM: (a) fluence = 0.95 J/cm^2, scale size = 200 nm.

DOI: 10.1021/acsami.5b09454
ACS Appl. Mater. Interfaces 2015, 7, 27467–27472

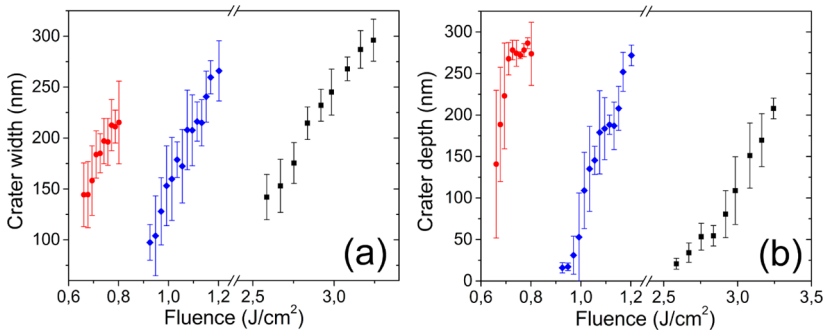

Figure 3. Averaged crater width (a) and depth (b) as a function of femtosecond pulse fluence: red circles, 2.25 μm microspheres; blue diamonds, 1.15 μm microspheres; black squares, no microspheres used.

consequence of focusing by dielectric spheres and corresponding intensity enhancement near spheres. Moreover, the threshold depended on femtosecond pulse polarization (Figure S1). Both the depth and width of craters were minimal near the processing threshold and increased with fluence growth (Figure 3). We defined fluence as a ratio of pulse energy to focal spot area; however, in experiments with microspheres the effect of intensity enhancement in the near-field produced a much larger local fluence near spheres. Crater FWHM dependence of laser fluence was approximately linear, whereas the crater depth demonstrated an obvious nonlinear dependence of fluence. The depth became very small (tens of nanometers and smaller) with fluence just above the processing threshold; however, we were able to produce only quite big craters with 2.25 μm microspheres (red circles, Figure 3a,b) even at threshold fluence. It is important to note that even near the processing threshold when the crater depth was approaching zero, craters could not be made smaller than a certain minimal size, which determined a practical resolution limit of our method. As seen from Figure 3a, this minimal resolution was best for 1.15 μm silica microspheres. From experimental data we conclude that maximal crater depth is limited by approximately 300 nm, and we have depth saturation for fluencies over 0.7 J/cm^2 for 2.25 μm microspheres (Figure 3b).

Minimal obtained crater dimensions are depicted in Figure 4. Craters had a nearly circular shape, although femtosecond pulse linear polarization ($\boldsymbol{E}$ along the OX-axis) tends to cause ellipticity of the near-field zone and the crater shape.[26,27] When femtosecond pulses were focused without microspheres and filled the whole input pupil of the objective lens (40× 0.75 N.A.), craters of a similar depth had FWHM of about 150 nm (Figure S2).

The fluence of femtosecond pulses also affected trap stability. Nonlinear absorption of femtosecond radiation in either glass or water produced electronic plasma and strong localized heating, which in turn could lead to shock wave formation and cavitation in water.[28] They disturbed optical trapping and caused displacement of the microspheres from the trap center, which we observed visually in experiments. This displacement was similar to the effects observed in microsphere-assisted ablation of polymer.[29] The amplitude of this movement was a strong function of pulse fluence. Near threshold fluencies this disturbance was barely detectable and manifested itself as a faint jitter of the microsphere. At higher fluencies the microsphere moved mainly in a vertical direction far from the sample surface but was then returned by optical forces to the trap center. The period of this movement was up to several seconds. Finally, we observed that at fluencies about 30% larger than processing threshold the microsphere was ejected so far that it did not return to its initial position and stayed far from the trap center. This effect determined an upper limit of practical fluence range we could use in microsphere-assisted processing.

Creating predefined structures is important for real applications; using optically manipulated microspheres we can easily transform computer-defined patterns to structures on the glass surface with resolution down to 100 nm. To illustrate this capability, an abbreviation for the Institute of Chemical Physics (ICP) written on the sample surface is shown in Figure 5. The optical trap is stable enough for accurate positioning of microspheres with high relative stage velocity approaching 5 μm/s. The pattern was written as a series of single holes with 50 nm minimal separation; laser fluence was equal to

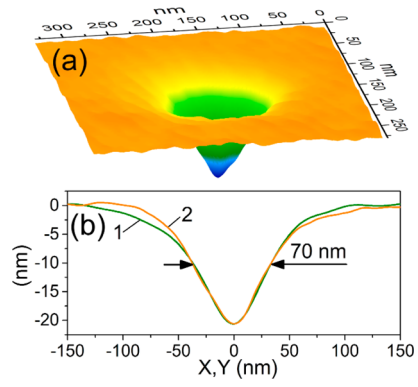

Figure 4. AFM image of the reproducible crater (a) and its cross sections (b): 1, along the X-axis; 2, along the Y-axis. The crater was produced with a 1.15 μm silica microsphere. Laser fluence = 0.93 J/cm^2.

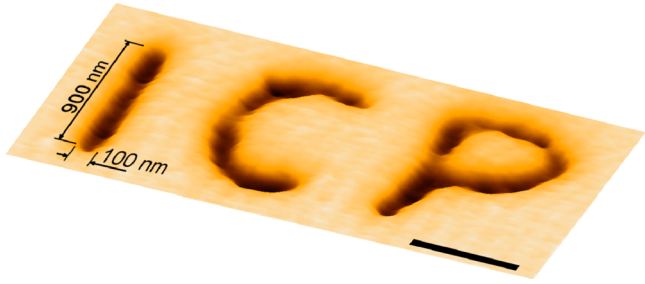

Figure 5. Two-dimensional image of ICP abbreviation on the borosilicate glass surface: scale size = 500 nm; mean groove depth = 20 nm; microsphere size = 1.15 μm; laser fluence = 0.98 J/cm^2.

DOI: 10.1021/acsami.5b09454
ACS Appl. Mater. Interfaces 2015, 7, 27467−27472

approximately 0.98 J/cm^2. The resulting pattern had a line width slightly larger than 100 nm and a groove depth of 20 nm. These results demonstrate how our technique can be applied for writing complex 2D patterns on sample surface with high spatial resolution.

We have examined focusing of laser pulses by dielectric microspheres theoretically. For this aim we used a MATLAB package (SPlaC v1_0),[30] which relies on Mie scattering theory. We calculated EM field intensity distribution inside and in the vicinity of a spherical dielectric particle illuminated by a plane linearly polarized wave. In simulations the refractive index of the particle was taken to be 1.46; medium, 1.33; and light wavelength, 780 nm. We neglected effects associated with finite spectral width of femtosecond pulses. Simulation results in the plane perpendicular to polarization are presented in Figure 6. The intensity distribution in the polarization plane is depicted in Figure S3.

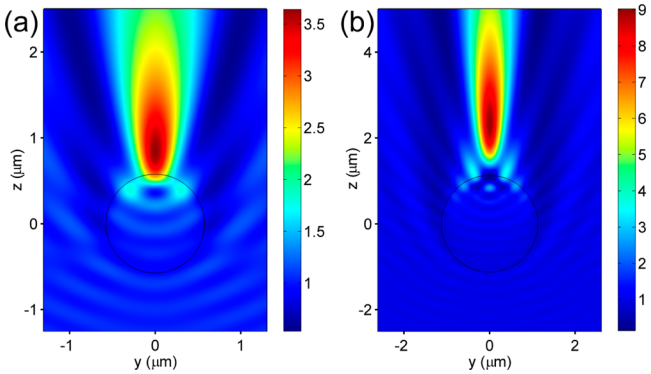

Figure 6. Simulated light intensity distribution around 1.15 μm (a) and 2.25 μm (b) silica microspheres illuminated by plane light wave; wavelength = 780 nm. Observation plane is perpendicular to the polarization (***E*** along the *OX*-axis).

The first result is the value of intensity enhancement, which is defined as the ratio of maximal intensity in the vicinity of the sphere to the intensity of the incident wave. Simulations show that the larger the sphere, the greater enhancement it produces. Thus, for a 1.15 μm silica sphere the enhancement factor is equal to about 3.5 (Figure 6a), whereas for 2.25 μm it is almost 9 (Figure 6b). We can compare these calculated factors with experimentally measured processing thresholds. As said previously, focusing of light by silica sphere decreased the threshold 2.8 and 3.9 times, respectively. Whereas the first value is in the range of the calculated enhancement factor, the second is obviously much smaller. To understand this disagreement, we should analyze intensity distribution patterns in Figure 6. For the smaller sphere the intensity maximum is located near the sphere, but for the larger 2.25 μm sphere it is at more than a micrometer distance from the surface. Consequently, in the latter case, the effective intensity, which influences processed material, would be considerably smaller than the maximal. Separation of intensity maximum from the sphere surface also means that radiation absorption can be concentrated some distance from the glass surface. That would explain why it was problematic to produce shallow craters with large (2.25 μm) silica spheres and the craters tended to have a large (about 200 nm) depth even for fluence slightly higher than the threshold (see Figure 3b)

Areas exposed to laser radiation change its chemical interaction with KOH. One possible reason is the formation of bumps through laser-induced swelling with altered global density and higher surface area. The other apparent reason is a change in glass chemical composition.

Amorphous silica glass has irregular ring structures with different numbers of Si atoms in the ring (from 2 to 6) along with a network of SiO_4 tetrahedra.[21,24] It is assumed local densification in LAZs happens due to compaction of large rings to the most compact two-membered rings. When all rings are converted, then first nanocracks or irreversible damage appears.[24] On the other hand, it was assumed that local change in chemical composition took place, when Si-rich centers (≡Si–Si≡), oxygen deficiency centers (=Si^0), color centers (≡Si$^\bullet$), and nonbridging oxygen-hole centers (≡Si—O$^\bullet$) formed in the LAZ.[21,22]

We performed TOF-SIMS imaging of bump arrays to visualize the change in chemical composition (Figure 7). In this experiment a 100 μm square area was processed with femtosecond pulses producing an array of surface bumps, separation between points was 1 μm, and laser fluence was 2.75 J/cm^2, and to clean the surface, the glass was pretreated in KOH for 1 min at 90 °C before the scan (Figure 7a,b).

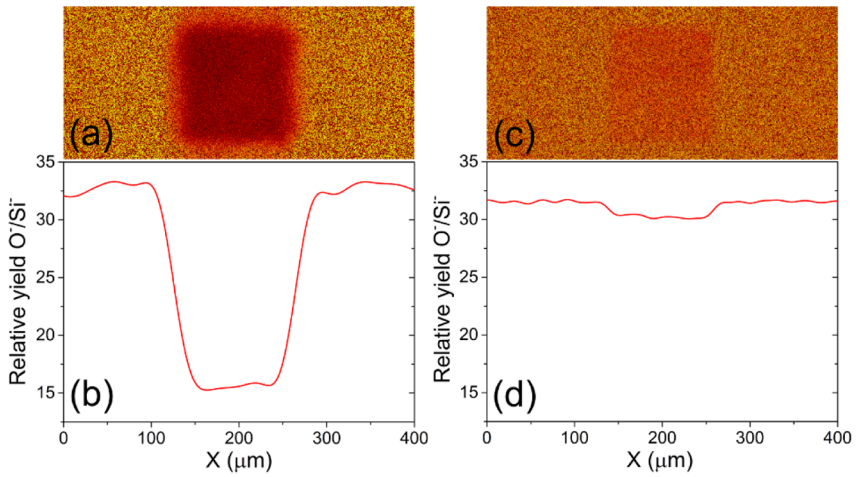

Figure 7. Maps of O$^-$/Si$^-$ ion ratio (a, c) and their averaged sections (b, d) from a region of fused silica glass exposed to femtosecond pulses before (a, b) and after (c, d) etching in KOH. Ion ratio was measured by a TOF-SIMS.

DOI: 10.1021/acsami.5b09454
ACS Appl. Mater. Interfaces 2015, 7, 27467−27472

To exclude topographical artifacts, we visualized the ratio of O^- to Si^- ion yield. As seen from Figure 7a,b laser treatment resulted in considerably lower (up to 50%) relative yield of O^- ions in the LAZ. When this sample was treated with KOH according to our standard procedure, the contrast mostly disappeared, although some decrease in relative O^- yield was registered on the processed square, it was not more than 5% (Figure 7c,d). One can conclude that laser exposure provides a change in chemical composition of the LAZ and their oxygen deficiency, which we observed on the mass spectrometry image. After treatment with KOH, the altered surface layer was mostly etched, uncovering material with normal oxygen content, which resulted in a lesser contrast image. We surmise the alteration in oxygen concentration can lead to the change in Si atoms arrangement and the appearance of Si-rich (O-deficiency) centers. Thus, noticeable oxygen deficiency could be the main reason why LAZ is etched more quickly than unaffected glass. On the other hand, oxygen release may lead to the formation of local voids or porous structures and may be responsible for the emergence of bumps on the surface. These changes may have extra action on the chemical reactivity of LAZ in glass.

CONCLUSION

We utilized a new technique involving near-field, optical trapping of silica microspheres and postprocessing in KOH to pattern borosilicate glass surface. Production of craters on the glass surface with diameters as small as 70 nm or less than one-tenth of light wavelength was demonstrated. Complex two-dimensional surface patterns were written point-by-point by translating the trapped microsphere by optical tweezers and were converted into concave structures after chemical etching. Mass spectrometry analysis of LAZ has evidenced a significant oxygen deficiency of the material that explains its selective chemical etching.

ASSOCIATED CONTENT

Supporting Information

The Supporting Information is available free of charge on the ACS Publications website at DOI: 10.1021/acsami.5b09454.

Figure S1, crater width as a function of femtosecond pulse fluence for different polarization; Figure S2, AFM image of the reproducible crater and its cross sections made without microsphere; Figure S3, simulated light intensity distribution around microspheres in polarization plane (PDF)

AUTHOR INFORMATION

Corresponding Author

*(A.S.) E-mail: physics2007@yandex.ru. Phone: 7 495 939 73 47.

Notes

The authors declare no competing financial interest.

ACKNOWLEDGMENTS

This work was financially supported by the Russian Academy of Science Presidium program 1 2015 ("Nanostructures") and by the Russian Foundation for the Basic Research in the part of theoretical studies and experimental measurements 14-03-00546 a, 13-02-12433 (ofi_m2). Young scientists A.A. and A.S. had financial support from Russian President Grant MK-5486.2014.2. The experimental setup was prepared with partial support from Russian Science Foundation Grant 14-33-00017.

REFERENCES

(1) Aeschlimann, M.; Bauer, M.; Bayer, D.; Brixner, T.; Garcia de Abajo, F. J.; Pfeiffer, W.; Rohmer, M.; Spindler, C.; Steeb, F. Adaptive Subwavelength Control of Nano-Optical Fields. *Nature* **2007**, *446*, 301−304.

(2) Kawata, S.; Sun, H. B.; Tanaka, T.; Takada, K. Finer Features for Functional Microdevices − Micromachines Can Be Created with Higher Resolution Using Two-Photon Absorption. *Nature* **2001**, *412*, 697−698.

(3) Betzig, E.; Trautman, J. K. Near-Field Optics: Microscopy, Spectroscopy, and Surface Modification Beyond the Diffraction Limit. *Science* **1992**, *257*, 189−195.

(4) Hwang, D. J.; Chimmalgi, A.; Grigoropoulos, C. P. Ablation of Thin Metal Films by Short-Pulsed Lasers Coupled through near-Field Scanning Optical Microscopy Probes. *J. Appl. Phys.* **2006**, *99*, 044905.

(5) Chimmalgi, A.; Grigoropoulos, C. P.; Komvopoulos, K. Surface Nanostructuring by Nano-/Femtosecond Laser-Assisted Scanning Force Microscopy. *J. Appl. Phys.* **2005**, *97*, 104319.

(6) Ohtsu, M.; Kobayashi, K.; Ito, H.; Lee, G. H. Nanofabrication and Atom Manipulation by Optical near-Field and Relevant Quantum Optical Theory. *Proc. IEEE* **2000**, *88*, 1499−1518.

(7) Zhang, J.; Li, Y.; Zhang, X.; Yang, B. Colloidal Self-Assembly Meets Nanofabrication: From Two-Dimensional Colloidal Crystals to Nanostructure Arrays. *Adv. Mater.* **2010**, *22*, 4249−4269.

(8) Piglmayer, K.; Denk, R.; Bauerle, D. Laser-Induced Surface Patterning by Means of Microspheres. *Appl. Phys. Lett.* **2002**, *80*, 4693−4695.

(9) Luk'Yanchuk, B. S.; Wang, Z. B.; Song, W. D.; Hong, M. H. Particle on Surface: 3D-Effects in Dry Laser Cleaning. *Appl. Phys. A: Mater. Sci. Process.* **2004**, *79*, 747−751.

(10) Pikulin, A.; Bityurin, N.; Langer, G.; Brodoceanu, D.; Baeurle, D. Hexagonal Structures on Metal-Coated Two-Dimensional Microlens Arrays. *Appl. Phys. Lett.* **2007**, *91*, 191106.

(11) Juodkazis, S.; Yamasaki, K.; Marcinkevičius, A.; Mizeikis, V.; Matsuo, S.; Misawa, H.; Lippert, T. Microstructuring of Silica and Polymethylmethacrylate Glasses by Femtosecond Irradiation for MEMS Applications. *MRS Online Proc. Libr.* **2001**, *687*, B5.25.

(12) Royer, P.; Barchiesi, D.; Lerondel, G.; Bachelot, R. Near-Field Optical Patterning and Structuring Based on Local-Field Enhancement at the Extremity of a Metal Tip. *Philos. Trans. R. Soc., A* **2004**, *362*, 821−842.

(13) Plech, A.; Leiderer, P.; Boneberg, J. Femtosecond Laser near Field Ablation. *Laser Photonics Rev.* **2009**, *3*, 435−451.

(14) Eversole, D.; Luk'yanchuk, B.; Ben-Yakar, A. Plasmonic Laser Nanoablation of Silicon by the Scattering of Femtosecond Pulses near Gold Nanospheres. *Appl. Phys. A: Mater. Sci. Process.* **2007**, *89*, 283−291.

(15) Bityurin, N.; Afanasiev, A.; Bredikhin, V.; Alexandrov, A.; Agareva, N.; Pikulin, A.; Ilyakov, I.; Shishkin, B.; Akhmedzhanov, R. Colloidal Particle Lens Arrays-Assisted Nano-Patterning by Harmonics of a Femtosecond Laser. *Opt. Express* **2013**, *21*, 21485−21490.

(16) McLeod, E.; Arnold, C. B. Subwavelength Direct-Write Nanopatterning Using Optically Trapped Microspheres. *Nat. Nanotechnol.* **2008**, *3*, 413−417.

(17) McLeod, E.; Arnold, C. B. Optical Analysis of Time-Averaged Multiscale Bessel Beams Generated by a Tunable Acoustic Gradient Index of Refraction Lens. *Appl. Opt.* **2008**, *47*, 3609−3618.

(18) Vishnubhatla, K. C.; Bellini, N.; Ramponi, R.; Cerullo, G.; Osellame, R. Shape Control of Microchannels Fabricated in Fused Silica by Femtosecond Laser Irradiation and Chemical Etching. *Opt. Express* **2009**, *17*, 8685−8695.

(19) Marcinkevičius, A.; Juodkazis, S.; Watanabe, M.; Miwa, M.; Matsuo, S.; Misawa, H.; Nishii, J. Femtosecond Laser-Assisted Three-Dimensional Microfabrication in Silica. *Opt. Lett.* **2001**, *26*, 277−279.

(20) Hnatovsky, C.; Taylor, R. S.; Simova, E.; Rajeev, P. P.; Rayner, D. M.; Bhardwaj, V. R.; Corkum, P. B. Fabrication of Microchannels in Glass Using Focused Femtosecond Laser Radiation and Selective Chemical Etching. *Appl. Phys. A: Mater. Sci. Process.* **2006**, *84*, 47−61.

DOI: 10.1021/acsami.5b09454
ACS Appl. Mater. Interfaces 2015, 7, 27467−27472

(21) Kiyama, S.; Matsuo, S.; Hashimoto, S.; Morihira, Y. Examination of Etching Agent and Etching Mechanism on Femotosecond Laser Microfabrication of Channels inside Vitreous Silica Substrates†. *J. Phys. Chem. C* **2009**, *113*, 11560−11566.
(22) Drevinskas, R.; Gecevičius, M.; Beresna, M.; Bellouard, Y.; Kazansky, P. G. Tailored Surface Birefringence by Femtosecond Laser Assisted Wet Etching. *Opt. Express* **2015**, *23*, 1428−1437.
(23) LoTurco, S.; Osellame, R.; Ramponi, R.; Vishnubhatla, K. C. Hybrid Chemical Etching of Femtosecond Laser Irradiated Structures for Engineered Microfluidic Devices. *J. Micromech. Microeng.* **2013**, *23*, 085002.
(24) Bellouard, Y.; Said, A.; Dugan, M.; Bado, P. Fabrication of High-Aspect Ratio, Micro-Fluidic Channels and Tunnels Using Femtosecond Laser Pulses and Chemical Etching. *Opt. Express* **2004**, *12*, 2120−2129.
(25) Hnatovsky, C.; Taylor, R. S.; Rajeev, P. P.; Simova, E.; Bhardwaj, V. R.; Rayner, D. M.; Corkum, P. B. Pulse Duration Dependence of Femtosecond-Laser-Fabricated Nanogratings in Fused Silica. *Appl. Phys. Lett.* **2005**, *87*, 014104.
(26) Astaf'ev, A. A.; Shakhov, A. M.; Oleg, M. S.; Nadtochenko, V. A. Microstructuring of Polymer Films by Femtosecond Pulses through Optically Trapped Polystyrene Microspheres. *Quantum Electron.* **2013**, *43*, 361−364.
(27) Shakhov, A. M.; Astafiev, A. A.; Plutenko, D. O.; Sarkisov, O. M.; Shushin, A. I.; Nadtochenko, V. A. Femtosecond Optical Trap-Assisted Nanopatterning through Microspheres by a Single Ti:Sapphire Oscillator. *J. Phys. Chem. C* **2015**, *119*, 12562−12571.
(28) Vogel, A.; Noack, J.; Huttman, G.; Paltauf, G. Mechanisms of Femtosecond Laser Nanosurgery of Cells and Tissues. *Appl. Phys. B: Lasers Opt.* **2005**, *81*, 1015−1047.
(29) Fardel, R.; McLeod, E.; Tsai, Y.-C.; Arnold, C. Nanoscale Ablation through Optically Trapped Microspheres. *Appl. Phys. A: Mater. Sci. Process.* **2010**, *101*, 41−46.
(30) Ru, E. L.; Etchegoin, P. *Principles of Surface-Enhanced Raman Spectroscopy: And Related Plasmonic Effects*; Elsevier Science, 2008.

DOI: 10.1021/acsami.5b09454
ACS Appl. Mater. Interfaces 2015, 7, 27467−27472